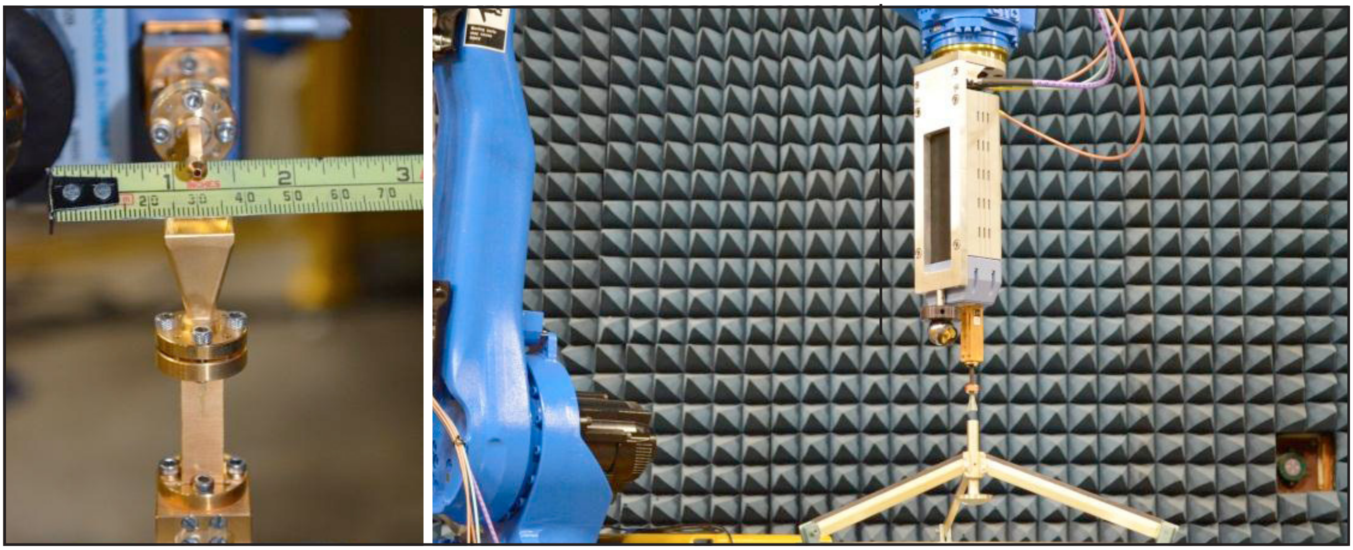

Use of a Laser Tracker to Actively Coordinate the Motion of a 3-Meter Industrial Robot to Within 50 Microns

by David Novotny, Joshua Gordon, Jason Coder, Jeff Guerrieri, and Michael Francis; National Institute of Standards and Technology

The Antenna Metrology Lab at the National Institute of Standards and Technology in Boulder, Colorado, is developing a robotically controlled antenna facility that uses industrial-grade robotics guided by a metrology-grade laser tracker to perform antenna calibrations over the frequency range 50 GHz to 500 GHz. These measurements are performed by scanning a millimeter wave (mm wave) probe antenna about a test antenna over an arc using an articulated six degree of freedom (6DoF) robotic arm that has a reach of 3 meters. Such near-field measurements yield important antenna parameters such as gain, polarization, and radiation pattern. Operation at 500 GHz requires knowledge of the probe antenna position to within 15–20 μm as well as orientation normal to the scan surface (typically within ~ 0.05°) to minimize pointing errors. Ultimately, our ability to accurately position and orient the probe antenna relative to the test antenna, as well as our knowledge of actual position and orientation, determine the upper frequency limit of our measurement capability, and directly affect the uncertainty of our measurements.

INTRODUCTION

We are designing a 50–500 GHz, multipurpose, antenna pattern and gain calibration range based on an industrial 6DoF articulated robot with a 3-meter reach, a precision (0.0001° resolution) azimuth rotator, and an alignment hexapod, as seen in figure 1. Antenna testing requirements are increasing in frequency above 110 GHz as high-speed satellite-to-satellite communications, short-range terrestrial point-to-point links, and absolute calibration techniques for remote sensing and climate monitoring research come to the forefront.[1] Our need to accurately position and align antenna under test (AUT) to fractions of a wavelength, and even more accurately know actual position during measurement, are driving forces in accurate coordinate measurement. Furthermore, the delicacy of equipment in these frequency ranges creates problems for physical contact by conventional (at least to the antenna measurement community) probing. Our eventual reliance on a combination and coordination of machine vision, movement methods, and positional measurement is forcing a new method of performing high-frequency antenna alignments and calibrations.

Current mm wave (above 100 GHz) antenna characterization facilities tend to focus on planar scanning techniques.[2] Planar scanning can give accurate pattern information over an approximate ± 30–35° angle range, is generally easier to align, requires less information about the radiation characteristics of the probe, and generally requires less complicated facilities. However, if accurate information is required beyond the central beam area, antenna efficiency is necessary (as in radiometer characterization), wide-angle polarimetric information is required, or full-pattern characterization of low gain antennas is needed, then other scan geometries, such as spherical or cylindrical, become more attractive.[3]

The use of a 6DoF robot for probe positioning and a laser tracker (with optional 6DoF measurement capability) for true positional measurements can provide the ability to perform multiple scan geometries, correct for positional and pointing errors in the AUT and probe, and determine actual *in situ* measurement positions to further improve overall result accuracy.[4] This coordinated 6DoF movement with independent 6DoF positional measurements might provide considerable reduction in uncertainty over conventional antenna characterization facilities that use stacked positional stages for each type of movement.

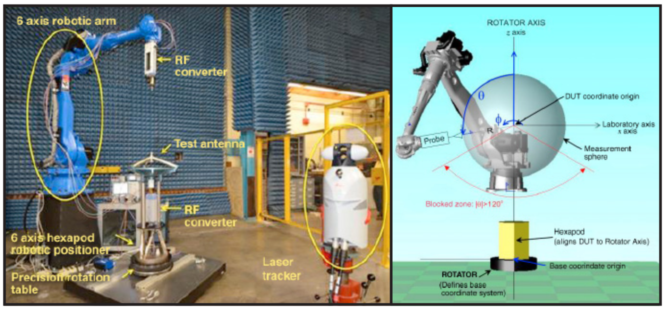

Figure 1. Physical (left) and conceptual (right) layout of the antenna characterization facility setup in spherical measurement mode, as the central axis of the rotator sets the location and orientation of the AUT's z axis and origin of the probe scanning; major tasks include aligning hexapod movement to rotator axis for AUT alignment, clocking AUT rotation to probe scan plane (AUT polarization), aligning probe rotation to probe scan plane and center (probe polarization), and correcting probe location for kinematic offsets in robot movement (mechanical position correction)

SYSTEM OVERVIEW

The task of accurately and repeatably moving a probe antenna over a desired path at these frequency ranges is complicated because physical contact with the antennas is problematic, the limited size of the antennas makes accurate angular alignment difficult, and the aperture origin is often virtual, so it must be inferred from measurements, as seen in the graphic at the top of this article. The extrapolations of the probe coordinate systems and alignment of the multiple coordinate systems (e.g., rotator, hexapod, AUT, robot, probe, and scan geometry) complicates the desired coordinate positioning and measurement between the probe and the AUT.

To accomplish the desired scanning process of the probe around the AUT, the antenna range is built on two major robotics platforms. The first section consists of AUT positioning and clocking mechanisms. In figure 1, the rotation stage sits upon an *xy* stage that nominally places the rotation center and AUT in an optimal position to get maximum angular coverage from the robot. By fixing the position of the *xy* stage, the rotation stage is fixed, as is the central *z* axis of the entire measurement. The 6DoF hexapod then aligns the AUT to the *z* axis, both in lateral translation and rotational pointing alignment. Once aligned to the rotator, the *z* origin for the AUT is established. The robot and probe must now be aligned to the AUT reference frame. The resultant series of stacked alignments produces systematic pointing and position errors that need to be addressed.[5]

ALIGNMENT

To accurately scan the probe around the AUT and to measure the radiating characteristics of the AUT, alignment of the multiple subsystem components must be performed.

Main *z* axis definition from rotator measurements

The rotator is scanned with a corner cube reflector (CCR) affixed to the rotator table (below the hexapod), as seen in figure 3. Propagation obstructions due to the hexapod and cabling limit single-mounting point CCR scans to approximately 200° scans of the θ rotation. We can validate that the out-of-plane table movement is acceptable (< 20 μm), and multiple scans show acceptable variations in the pointing of the *z* axis (< 0.008°). It is imperative that the rotator measurement be as accurate as possible. It is the virtual baseline by which all the other alignments are based. Taking large numbers of points over as large a physical distance as possible is required to minimize the fitting errors of the central axis.

Hexapod coordinate system definition

The absolute origin of the hexapod coordinate system was determined by measuring three arcs trajectories of a mounted CCR on the hexapod plane while the hexapod was commanded through its angular range of motion about the three angles, *Rx*, *Ry*, and *Rz*. These angles each correspond to movement about the *x*, *y*, and *z* Cartesian axes, respectively. Full circles were then fitted to these arcs and the normal of these circles determined. From the intersection of the three circle normals, the origin and orientation of the hexapod frame could be determined. In addition, movement of the hexapod along its three Cartesian coordinates relative to the $x = 0$, $y = 0$, and $z = 0$ home position verified the proper orientation and direction of the three axes. With this, the full hexapod frame seen in figure 4 was established, which allowed for information about the movement of the hexapod relative to the laser tracker and other frames in the system.

AUT aperture coordinate definition and alignment to the *z* axis

The AUT aperture edges are measured and the centroid of the rectangular aperture is found, as seen in figure 5. A working frame is made at the centroid of the measured AUT aperture. The *z* axis of the AUT must be translated and rotated to be co-linear with the central *z* axis of the rotator. An ideal AUT frame is then erected as a goal frame, and the hexapod is used to guide the AUT. Based on a transformation between the measured AUT frame and the goal frame, a 6DoF set of offsets can be calculated by which to translate and rotate the hexapod, thereby aligning the AUT to the goal frame.

First, three widely spaced points on the hexapod plane are measured (relative to the AUT aperture to hexapod distance) from which an identical set of these three points is generated, but which are moved according to the AUT-to-goal transform. Two new frames are created from the first set of three points and a second translated set, respectively. The transform between these two new frames is then calculated to give the final *x*, *y*, *z*, *Rx*, *Ry*, and *Rz* coordinates to which the hexapod must be translated to align the AUT to the *z* axis of the rotator. The result of applying the AUT-to-goal transform can be seen in figure 6.

The three reference points are translated until the calculated AUT centroid is aligned with the central *z* axis. Errors can accumulate here, as the AUT-to-reference-point distance is large compared to the basis for the hexapod coordinate frame. To minimize these translation errors, the aperture needs to be measured again to verify the alignment of the aperture after the move.

Robot coordinate system definition

Once the AUT is aligned to the rotation stage and the central *z* axis, robot alignment can be performed. The robot movement needs to be coordinated with the laser tracker. There are two

Component	Task(s)	Nominal figures of merit
Rotation stage	• Sets central z axis of the entire measurement system • Provides ϕ rotation of the AUT • Sets polarization reference of the AUT	• Better than 20 μm flatness • 3,600,000 steps/rotation (0.0001°) • Repeatability better than 0.0005°
Hexapod	• Provides 6DoF alignment between AUT and central z axis	• Allows virtual pivot point alignment relative to AUT center • <1 μm resolution • 50 mm/±15° travel • 30 kg AUT capacity
6DoF robot	• Provides scan geometry (θ scan about AUT for spherical, 2D scan plane for planar) for the probe • Aligns scan geometry to z axis • Provides probe polarization • Full 6DoF movement allows software correction of actual measurement position	• 30 kg load capacity (includes probe, mm wave hardware, supports, and cabling • ±70 μm rated repeatability (not accuracy) • 3-m reach can provide up to 1.25-m measurement radius at the probe aperture • Up to 1.5 x 2 m planar scan size
Laser tracker	• Measures 3D position data • With three nonlinear CCRs, accurate stationary 6DoF can be measured • 6DoF sensors can measure in real time at moderates speeds (<1 m/s)	• Within the 2–3 m working range, repeatability and accuracy < 20 μm for direct CCR measurement • 6Dof sensor ± 0.01° (18 μm/ 100 mm) pointing error and 50 μm positioning error relative to central reflector

Figure 2. Table showing subsystem specifications of the NIST mm wave antenna measurement range

obvious methods of performing the frame translations between the robot and the laser tracker. We can create a frame similar to the hexapod movement of the AUT. We can also move the robot in its base *x*, *y*, and *z* motions to calculate a virtual laser tracker frame for the base robot movement that can be translated relative to the AUT frame. This will allow the altering of the robot geometry to match the scanning needs of the AUT in base robot coordinates. This allows for less error-prone movements when shifting a large robot around small, sensitive, and fragile objects.

Additionally, timing between the robot and the laser tracker must be coordinated. The robot movement to a given position must be coordinated with the laser tracker capture of the position data and a measurement of the radiated energy between the AUT and probe antennas.[6] The robot motion needs to be continuous; if the robot is stopped at each measurement point, the cables that phase-lock the mm wave measurements continue to vibrate and cause errors. In this scenario, a pause must be inserted at each point (1–2 seconds) to allow for the system to stabilize prior to measurement. This can cause a 250,000-point scan to have an additional 80 hours of measurement time (the number of points tends to scale as the square of frequency). We have found that as long as the movement of the probe is less than 1/50th of the measurement, wavelength during the mm wave measurement the error due to movement is generally acceptable. This limits probe movement to approximately 30 millimeters/second for measurements at 100 GHz.

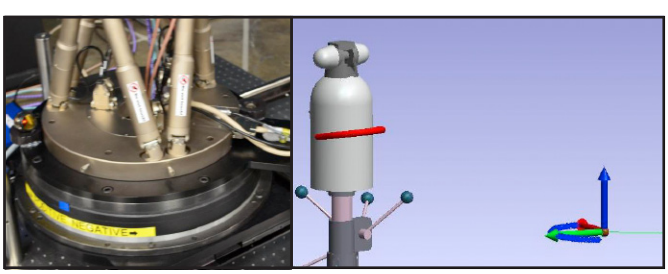

Figure 3. Determining the central z axis of the system: a CCR is placed on the rotation stage and moved through the maximum rotation without blockage to the laser tracker from the hexapod and cabling; the accurate determination of the vertical z axis (right) is critical to the accuracy of the entire measurement, and every component is aligned to the rotation stage

The robot has the ability to send a pre-trigger prior to arriving at a given point. A pulse can be sent out prior to arriving at the target point, to within the process timing cycle accuracy of the robot (~ 3 mS). This allows the positional placement, mm wave signal capture, and measurement of position to occur with minimal timing differences. The timing is initially estimated by robot speed. For a spherical scan of an AUT, the robot is scanned about the AUT, the AUT is rotated, and then the robot reverses its path. As seen in figure 7, we adjust the pre-triggering of the robot and delay of the instrumentation to ensure the data points are taken at the same point on the forward and reverse paths.

Once the basic timing of the robot is established, the robot is measured in its native *x*, *y*, and *z* movement, and a reference robot frame is established. This allows the errors in robot position to be translated directly into correction vectors in robot-coordinate space. As seen in figure 7, the robot repeatability at this speed is approximately 30 μm with a few outliers around 100 μm.

Probe coordinate system definition

One of the most difficult alignment tasks is the determination of the probe location and pointing relative to the robot and relative to the AUT. As seen in the figure at the top of the article, the probe can be delicate, and the force of a CCR being pressed against it can cause damage. We are developing a combination of machine vision techniques with a 6DoF offset sensor

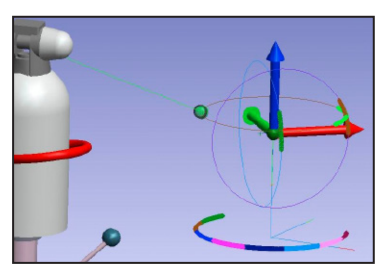

Figure 4. By moving the hexapod in its base coordinate x, y, z, Rx, Ry, and Rz motions, a coordinate frame relative to the hexapod can be established; this allows for direct calculation of the AUT translation needed to align it to the central z axis in hexapod coordinates

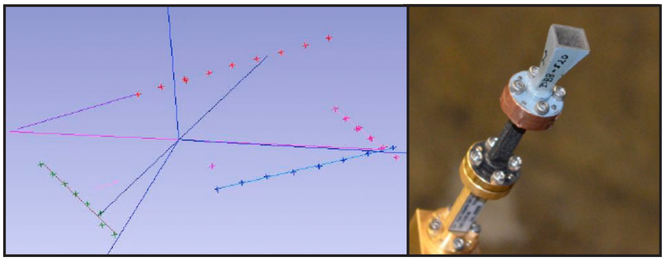

Figure 5. *Measurement of the initial position of the aperture: the AUT aperture is approximately 8 mm × 12 mm, and the initial position is measured relative to the rotator and hexapod frame; the lone point in the left graph is where the central z axis of the rotator intersects the plane of the aperture, while the frame of the aperture plane is seen as an offset from this ideal aperture location*

to determine probe location and orientation.[7] For verification of the positioning capability of the probe, a CCR is placed at the probe location, and a 6DoF sensor is offset approximately 250 millimeters away from the CCR. The CCR is driven to a given location to within robot step capability (~ 17 μm) from several different directions. The laser tracker measures the CCR in addition to the 6DoF sensor location and orientation. The robot joint set is also measured. The alignment of the probe tip relative to the 6DoF sensor and the robot tool interface are simultaneously measured. The knowledge of both of these offsets allows for first-order positioning and attitude control of the mm wave probe by the robot, and accurate measurement of the probe location and attitude by the 6DoF sensor.

To validate the alignment and accuracy of the 6DoF sensor relative to the laser tracker, the probe is scanned in the same arc used for the timing analysis. At each point in the forward and reverse arc, the 6DoF sensor is measured, and then the arc is repeated while measuring the CCR. Figure 8 demonstrates the differences between the probe position as measured by the CCR and 6DoF sensor. The measured differences are consistent with the manufacturer specifications seen in

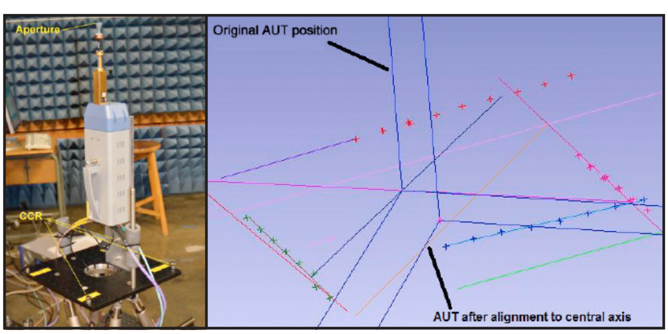

Figure 6. *Aperture translation and rotation via the hexapod: the calculation of the frame-to-frame translations between initial and desired position in the hexapod movement frame allows for direct hexapod movement relative to its base coordinates; the translation between the aperture and the base plate is done by measuring three nonlinear points on the base plate relative to the initial aperture position, and an iterative translation was done; post-alignment verification of the AUT aperture shows that alignment of the AUT to the central z axis is within ± 30 μm and ± 0.04°*

the table in figure 3, and the offset between the sensor and probe. The robot process timing accuracy of 3 mS may account for the outliers around 100 μm. Occasionally (< 0.5%) the robot may take an additional timing interval to process information; this additional 3 mS at a 30 mm/s velocity translates to a 90 μm offset. The robot may to be going to the programmed point much closer than figure 8 suggests for the 100 μm to 130 μm; there is just a slight variation in the pre-trigger delay from the robot, causing the tracker and RF equipment to trigger at a slightly different delay.

Scan geometry alignment to the *z* axis and AUT aperture

The last alignment step prior to the actual measurement is to align the scan geometry to the *z* axis of the rotator and AUT aperture. The measurement arc is roughly located over the *z*-aligned AUT by measuring the initial, uncorrected arc path and calculating the centroid of the path. The arc is moved, in robot coordinates, to be centered on the AUT aperture, as seen in figure 9. No corrections are initially made for scan tilt relative to the AUT. Once a rough alignment is done (within ~ 300 mm), a scan is performed in both directions while capturing the probe position and probe-pointing orientation. The AUT is then rotated to achieve alignment with the scan frame using the central rotator, and the $\phi = 0°$ coordinate for the measurement is set.

This is where the 6DoF coordinated movement of the robot has markedly attractive advantages over current systems. The robot can correct 6DoF position and pointing errors simultaneously. The initial errors are relatively large (on the order of 10–20 millimeters), mainly due to the installation tilt of the robot relative to the rotator. The errors in the positions and attitudes of each

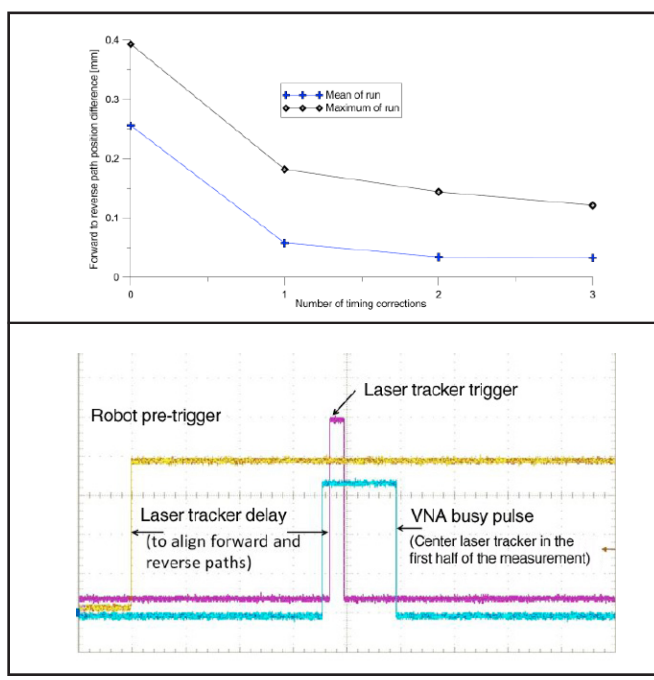

Figure 7. *Timing between the robot and the laser tracker: by adjusting the pre-trigger delay of robot and the tracker data acquisition delay (left), the relative position error between the forward and reverse scans can be minimized; once the tracker delay is set (right) the mm wave measurement is delayed to align to the laser tracker position capture*

individual measurement point is calculated, and the corrections (in the robot frame of movement) required to bring them to ideal are determined and sent back to the robot-positioning software. The first iteration of the corrections, as seen in figure 10, demonstrate that the measured error in the AUT frame is reduced to approximately 85 μm. Subsequent corrections can bring the mean positioning error to ~ 25 μm. We see little improvement after three rounds of positional iterations.

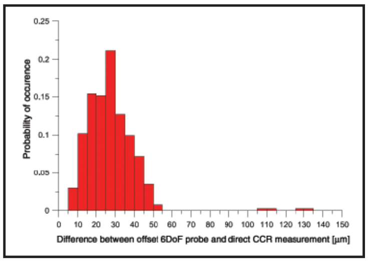

Figure 8. Measured differences between the same scan performed with an offset 6DoF sensor measuring probe position and a CCR directly measuring probe position: the start and stop points of the scan cluster is mainly between 40 µm and 50 µm; the few points above 100 µm may be related to timing uncertainty in the robot, as they do not repeat in location over repeated runs; it should be noted that the differences seen here are due to both the 6DoF sensor pointing errors and the robot repeatability seen in figure 7; currently, this is one of the larger sources of positional uncertainty and is limiting the operation of the system to ~ 250 GHz

The resulting errors can be corrected, to first order, using position correction techniques.[8] The time it takes to align the scan geometry is trivial compared to that for the AUT to rotator. In less than 30 minutes, four iterations of 6DoF position corrections were completed for the 802-point scan. Once the probe-to-6DoF-sensor offset is established, the corrections can be done for any scan geometry. Aligning within the 0.01° uncertainty of the 6DoF sensor provides the ability to have acceptable probe pointing errors for the low and moderate gain horns we use for probes. This is particularly important because pointing errors cannot be addressed by current processing methods.

Figure 11 demonstrates the corrected arc aligned to the AUT. The average positioning errors, including 6DoF sensor errors, are approximately 40 μm. The ϕ (rotator) axis is clocked to the scan plane, and the 0° point of the robot scan (ϕ axis) is aligned with the z axis of the rotator.

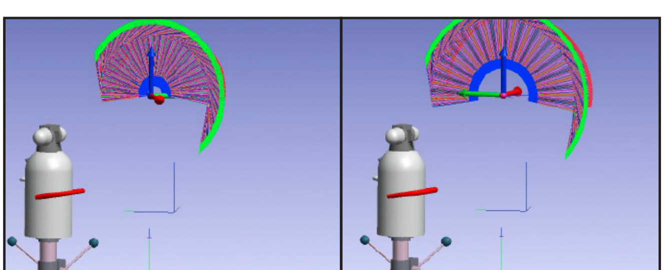

Figure 9. The first step of aligning the scan geometry of the probe to the AUT: the measured center of the uncorrected scan (left) is offset to approximately match the AUT location by moving the entire ensemble by a constant 6DoF offset; this results in an arc (right) with a positional variation of ~ 200 µm from ideal

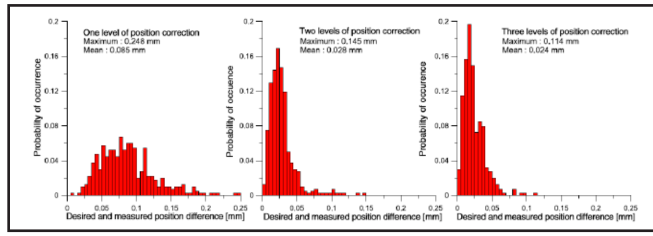

Figure 10. The effects of successive levels of position correction: we can see the 90 µm positioning error due to robot timing clearly once the mean error drops below 30 µm, and we can implement position correction techniques to minimize the error of these outliers if they constitute a small portion of the total scan area or received power from the AUT; this error is independent of the 6DoF offsets in figure 8

POSITIONAL UNCERTAINTY ANALYSIS

Figure 12 demonstrates the basic background "noise" we see in positioning. The robot is stopped and there is no power to the motors, with the breaks on each axis. The resultant variation may be due to the floor moving, instability in the robot or laser track mounts, or the positional noise of the laser tracker itself. This represents a basic measurement limitation of the current setup. The raw position error/uncertainty/repeatability of the robot, as seen in figure 13, can be corrected to first order because the laser tracker is recording the actual position of the individual mm wave measurement. Currently the position uncertainty between the probe and the AUT can be estimated by the error in the probe as seen in figures 8 and 10. The root-sum-square (RSS) of the position displacements and the 6DoF sensor uncertainty is ~ 40 μm. However, better estimation of the actual probe and AUT aperture planes is needed. Measuring over a small surface and then extending the results to 100 times the length of measurement will lead to errors. The base error of the rotation stage as well as how it affects the alignment of the AUT frame and robot scan geometry needs to be assessed.

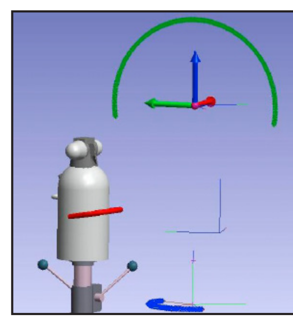

Figure 11. Resultant measurement points for spherical scanning of an AUT: the scan points are fitted to a planar-circular arc, and the nominal mean AUT to probe position errors of ~ ± 40 µm; this does not include the systematic offset of the measured probe and AUT frames from the actual position and points of the antennas; timing between the robot, positional tracking systems, and the measurement have been minimized to limit errors due to the robot movement during scanning, and many of the measured errors and offset from desired positions can be mitigated with position correction

FUTURE WORK

The most difficult tasks are defining the AUT aperture plane and the probe aperture plane. Work is underway to accurately determine the actual position and orientation of the aperture of the AUT and the probe; this should generate more accurate methods of determining the antenna center for location and antenna edges for determining orientation.[7] We will be assessing the possibility of stepping the robot and scanning the rotator. However, that puts more stress and strain on the RF cabling beneath the AUT. In this configuration, however, we can use three CCRs to align the probe tip, similar to the hexapod-to-AUT alignment. It may result in better probe aperture determination (down to the level of the base laser tracker error).

CONCLUSION

We presented a method for controlling the probe position of a scanning antenna system to within 50 μm relative to a centrally defined antenna coordinate system. It is the first stage in a complex alignment consisting of multiple stages. Once a basic scanning surface is defined, positional scanning errors can be corrected to half a wavelength. We can mathematically correct, to first order, the positioning error of the 6DoF robot (~ 40 μm). The ~ 50 μm error in the 6Dof sensor can be reduced by placing the sensor closer to the actual probe tip location. This possibly results in a reduction of sensor errors to 30 or 40 μm. These uncertainties in position may allow us to achieve the 1/25th of a wavelength acceptable error to approximately 300 GHz. The tasks of performing more robust 6DoF sensor-to-probe-tip alignment and AUT determination are the major hurdles still to overcome.

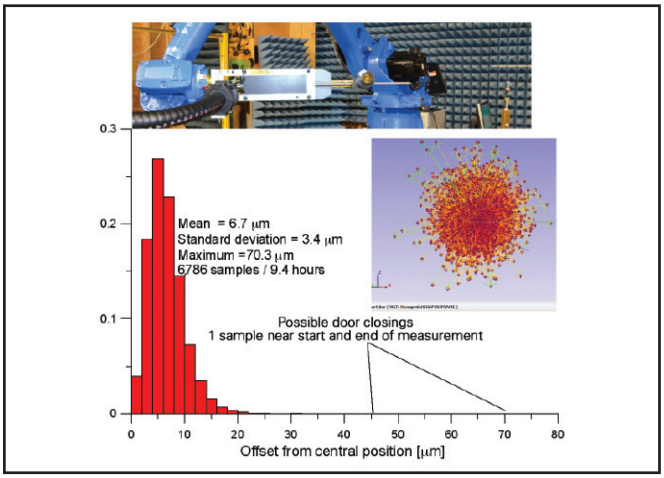

Figure 12. Nominal movement of the robot with respect to the tracker when the robot is not moving and has brakes engaged; motion in the room can be seen as outliers in these data; the point cloud on the left shows uniformity of the movement with time

REFERENCES

1 "Achieving Satellite Instrument Calibration for Climate Change (ASIC3);" Ohring, G. (ed.); National Oceanic and Atmospheric Administration; 2007.

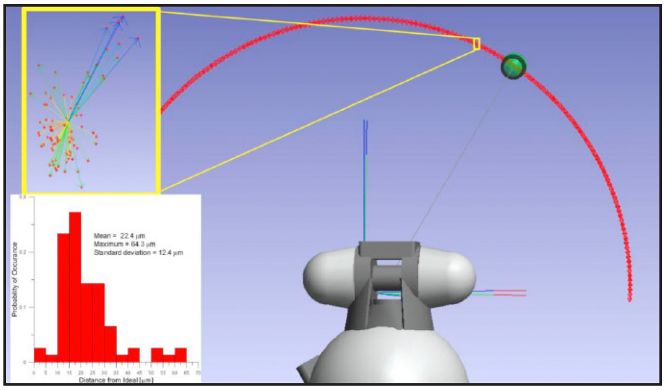

Figure 13. Nominal position spread for a single commanded position on the measurement arc for 71 sweeps of that point; mean deviation from ideal is ~ 22 µm with a maximum deviation of ~ 64 µm

[2] Slater, D., Hardy, J., Stek, P., Cofield, R., Dengler, R., Jarnot, R., and Swindlehurst, R.; "A Large Aperture 650 GHz Near-Field Measurement System for the Earth Observing System Microwave Limb Sounder;" *2001 Proceedings of the Antenna Measurement Techniques Association*; pp. 468–473; 2001.

[3] Hindman, G., Newell, A., Dicecca, L., and Angevain, J.C.; "Alignment Sensitivity and Correction Methods for Millimeter-Wave Spherical Near-Field Measurements"; *2010 Proceedings of the Antenna Measurement Techniques Association*; pp. 316–321; 2010.

[4] Rousseau, P., Wysock, W.C., and Turano, C.M.; "Using a Tracking Laser Interferometer to Characterize the Planarity of a Planar Near-Field Scanner"; *2002 Proceedings of the Antenna Measurement Techniques Association*; pp. 501–506; 2002.

[5] Francis, M. and Wittmann, R.; "Uncertainty Analysis for Spherical Near-Field Measurements"; *2003 Proceedings of the Antenna Measurement Techniques Association*; pp. 43–51, 2003.

[6] Novotny, D., Gordon, J., Coder, J., Francis, M., and Guerrieri, J.; "Performance Evaluation of a Robotically Controlled Millimeter-Wave Near-Field Pattern Range at NIST"; *Seventh European Conference on Antennas and Propagation*; pp. 4086–4089; 2013.

[7] Gordon, J., Novotny, D., Coder, J., Guerrieri, J., and Francis, M.; "Performance of a Robotically Controlled Near-Field Pattern Range in a Spherical Scan Geometry"; 2013 *Antenna Measurement Techniques Association;* 2013.

[8] Wittman, R., Alpert, B., and Francis, M.; "Planar Near-Field Antenna Measurements Using Non-Ideal Measurement Locations"; *1996 Proceedings of the Antenna Measurement Techniques Association;* pp. 74–79; 1996.